

Measurements of photo-nuclear jet production in Pb+Pb collisions with ATLAS

Aaron Angerami on behalf of the ATLAS Collaboration¹

Columbia University, New York, NY 10027, USA

Abstract

Ultra-peripheral heavy ion collisions provide a unique opportunity to study the parton distributions in the colliding nuclei via the measurement of photo-nuclear jet production. An analysis of jet production in ultra-peripheral Pb+Pb collisions at $\sqrt{s_{NN}} = 5.02$ TeV performed using data collected with the ATLAS detector in 2015 is described. The data set corresponds to a total Pb+Pb integrated luminosity of 0.38 nb^{-1} . The ultra-peripheral collisions are selected using a combination of forward neutron and rapidity gap requirements. The cross-sections, not unfolded for detector response, are compared to results from PYTHIA Monte Carlo simulations re-weighted to match a photon spectrum obtained from the STARLIGHT model. Qualitative agreement between data and these simulations is observed over a broad kinematic range suggesting that using these collisions to measure nuclear parton distributions is experimentally realisable.

Keywords: UPC, photoproduction, jets, nuclear parton distributions

1. Introduction

In the past few decades significant interest has developed on the subject of nuclear parton distribution functions (PDFs) and their modifications relative to the proton PDFs. In particular the possible connection between the suppression of nuclear PDFs at small values of x (shadowing) and non-linear evolution of the PDFs at large parton density [1, 2, 3] has received significant theoretical attention. A method for studying nuclear parton distributions using photo-nuclear production of dijets was proposed a decade ago [4, 5]. The intense electromagnetic fields accompanying the ions can be viewed as beams of quasi-real photons with energies distributed according to the Weizsäcker-Williams spectrum. Photons with wavelengths of order the size of the nucleus, R_N , are emitted coherently by the entire nucleus, and the flux is enhanced by a factor of Z^2 compared to the flux in pp collisions. For ultra-relativistic ion beams, the large longitudinal boost means the photons can have energies up to $E_\gamma \lesssim \sqrt{s_{NN}}/2m_N R_N \sim 40 \text{ GeV}$ at the LHC. Such photons have sufficient energy to stimulate hard-scattering processes and can thus resolve the partonic structure of the nucleus.

Processes may occur in which virtual excitations of the photon are probed by the hard interaction. In these “resolved” events the photon serves as a source of partons and only a fraction of the photon’s four-momentum contributes to the hard scattering. Hard photo-production was studied extensively at HERA,

¹A list of members of the ATLAS Collaboration and acknowledgements can be found at the end of this issue.

where the interplay between the direct and resolved contributions was exploited to study the partonic structure of both the proton and the photon [6, 7].

This process is one of many types of photon-induced reactions that are referred to as “ultra-peripheral collisions” (UPCs) because they can occur when the impact parameters between the incoming nuclei are large such that there is no hadronic interaction between the nuclei. In hadronic nuclear collisions the net color exchange gives rise to particle production that usually populates the entire rapidity region. As the photon carries no color, it is expected that photon-induced reactions will be accompanied by a *rapidity gap* in the the direction of the photon-emitting nucleus, although the gap may be reduced in size in the case of resolved events. Furthermore, the photon-emitting nucleus is expected to remain intact resulting in no neutrons along the beam direction, while multiple neutrons are expected in hadronic collisions due to the nuclear breakup.

These proceedings present a measurement of photo-nuclear jet production cross-sections in Pb+Pb collisions at a per nucleon center-of-mass energy of $\sqrt{s_{NN}} = 5.02$ TeV, recorded in 2015 [8]. Photo-nuclear events are identified by requirements on the number of neutrons and the presence of rapidity gaps. Specifically, events are required to have zero neutrons in one direction and one or more neutrons in the opposite direction, referred to as the “0nXn” event topology. The photon going direction is defined to be the direction in which zero neutrons are observed. Jets are reconstructed using the anti- k_t algorithm [9] with $R = 0.4$. The jets are used to construct per-event observables H_T , x_A and z_γ , which are defined in Section 3, and the cross-sections are measured differentially as a function of each of these variables. The cross-sections are not unfolded for detector response. In the limit of $2 \rightarrow 2$ scattering kinematics, x_A corresponds to the ratio of the energy of the struck parton in the nucleus to the (per nucleon) beam energy and $H_T \rightarrow 2\sqrt{Q^2}$, where Q^2 is the invariant momentum transfer in the hard scattering. The variable $z_\gamma = x_\gamma y$, where y is the energy fraction carried by the photon. For direct processes x_γ is unity, while for resolved events it is the fraction of the photon’s energy carried by the resolved parton entering the hard scattering.

2. Data and Monte Carlo samples

The measurements described in these proceedings are performed using the ATLAS detector [10] in the Run 2 configuration. They rely on the calorimeter system, the inner detector, the zero degree calorimeters, and the trigger system. The zero degree calorimeters (ZDCs), which measure neutrons emitted at small rapidity separation from the incident nuclei, were used for triggering and for offline event selection. The ZDCs are located a distance of 140 m on either side of the nominal interaction point and cover $|\eta| > 8.3$. Events are selected by a ZDC XOR trigger in which one of the ZDCs is required to have an energy deposit consistent with one or more neutrons while the opposite side ZDC was required to be consistent with zero neutrons.

To evaluate the impact of the detector response on the measured cross-sections, a Monte Carlo (MC) sample of events is used. The sample uses the PYTHIA event generator version 6.41 [11] with the Perugia2012 tune [12] configured for $\gamma^* + p$ collisions with the photons produced via bremsstrahlung from a muon beam. It uses the CTEQ6L1 proton PDF set and the SaS 1D photon PDFs [13, 14] and is configured to contain a mixture of direct and resolved processes. The generated events are passed through a GEANT4 [15] simulation of the ATLAS detector response [16] and analyzed in the same manner as ATLAS data. Events produced in this fashion do not have the appropriate photon flux for Pb beams. To account for this a weighting is applied as a function of photon energy on an event-by-event basis. The weighting is obtained by comparing the photon distribution in PYTHIA with that using the STARLIGHT [17] generator, which contains a description of the equivalent photon flux for ions. The per-jet and rapidity gap distributions in the reweighted sample, referred to as PYTHIA+STARLIGHT for the duration of these proceedings, agree well with data.

3. Data analysis

The rapidity gap analysis proceeds by applying the same selections on calorimeter clusters that are applied in other ATLAS measurements [18]. The resulting clusters and the charged particle tracks are

ordered in η and intervals between adjacent tracks or clusters with separation $\Delta\eta > 0.5$ are recorded. The sum of such gaps that lie between the largest- η and smallest- η jets and the closest detector boundary are determined and on both the photon-going and Pb-going sides of the detector will be referred to as $\sum_\gamma \Delta\eta$, and $\sum_A \Delta\eta$, respectively.

Events used in the measurement are required to satisfy the 0nXn condition in the ZDCs and to have $\sum_\gamma \Delta\eta > 2$ and $\sum_A \Delta\eta < 3$. The former requirement distinguishes UPC events from hadronic nuclear collisions while the latter requirement reduces background from $\gamma\gamma$ collisions and non-photo-nuclear UPC processes. Events are required to have a reconstructed vertex and at least one charged particle track passing applied selections if at least one of the jets falls within the inner detector acceptance. Corrections are applied to account for signal events removed by these requirements, and thus they are not part of the fiducial definition of the measurement.

Event-level observables are constructed from all jets having transverse momentum $p_T > 15$ GeV and pseudo-rapidity $|\eta| < 4.4$. Events are required to have two or more such jets and at least one jet with $p_T > 20$ GeV. The jets are used to define the event-level variables:

$$H_T \equiv \sum_i p_{Ti}, \quad m_{\text{jets}} \equiv \left[\left(\sum_i E_i \right)^2 - \left| \sum_i \vec{p}_i \right|^2 \right]^{1/2}, \quad y_{\text{jets}} \equiv \frac{1}{2} \ln \left(\frac{\sum_i E_i + \sum_i p_{zi}}{\sum_i E_i - \sum_i p_{zi}} \right), \quad (1)$$

where i runs over the measured jets in an even. The signs of p_z are chosen to be positive in the photon-going direction. A further requirement is imposed that the jet-system mass, m_{jets} , satisfies $m_{\text{jets}} > 35$ GeV. The differential cross-sections are measured as a function of H_T and

$$z_\gamma \equiv \frac{m_{\text{jets}}}{\sqrt{s}} e^{+y_{\text{jets}}}, \quad x_A \equiv \frac{m_{\text{jets}}}{\sqrt{s}} e^{-y_{\text{jets}}}. \quad (2)$$

Systematic uncertainties in the measured cross sections from uncertainties in the jet energy scale (JES) and jet energy resolution (JER) are evaluated by applying variations to reconstructed jet p_T values in the MC sample and considering the fractional change in the resulting cross section. The JER uncertainty is evaluated by adding additional p_T smearing to account for possible under-estimation of the JER in the MC sample. The evaluation of the JES uncertainties follows from the data-driven procedure used to obtain the calibrations applied to the jets in the analysis [19, 20]. For each jet in the MC sample, the four-momentum was varied according to 76 nuisance parameters, resulting from statistical and modeling uncertainties in the calibration procedure. Additional sources of systematic uncertainty arise from the luminosity measurement (6.1%) and various trigger and event selection efficiency corrections. The uncertainty on these corrections is typically less than a few percent, except at the largest values of z_γ .

4. Results

The measured cross-sections are shown in Fig. 1 as functions of x_A and z_γ , in the left and right panels, respectively. The cross-sections are shown for different ranges on H_T , scaled by successive powers of 10 for presentation purposes. Systematic uncertainties on the cross-sections due to event selection efficiency and jet response are shown on the figures with shaded bands. Not indicated on the figures is an overall systematic uncertainty on the normalization of 6.2% (luminosity and a subset of the event selection corrections). The corresponding cross-sections obtained from the PYTHIA+STARLIGHT sample, normalized to have the same integral as the data over the measured kinematic range, are also shown with dashed lines.

The agreement between data and Monte-Carlo is good over most of the range of the measurement, though it is less good at the largest and smallest z_γ and x_A values where the cross-sections are particularly sensitive to the kinematic selections in the analysis. Perfect agreement between data and PYTHIA+STARLIGHT should not be expected because of the known nuclear PDF modifications and because the PYTHIA+STARLIGHT MC sample did not include a sample of photon-neutron events with proper isospin averaging. Nonetheless, the fact that the data and MC agree over a wide range of z_γ and x_A show that the original proposal to study nuclear parton distributions in ultra-peripheral photo-nuclear collisions [4, 5] is realisable, that the resulting cross-sections reflect the expected photon spectrum, and that an event generator is capable of accurately describing the events and the jet kinematics.

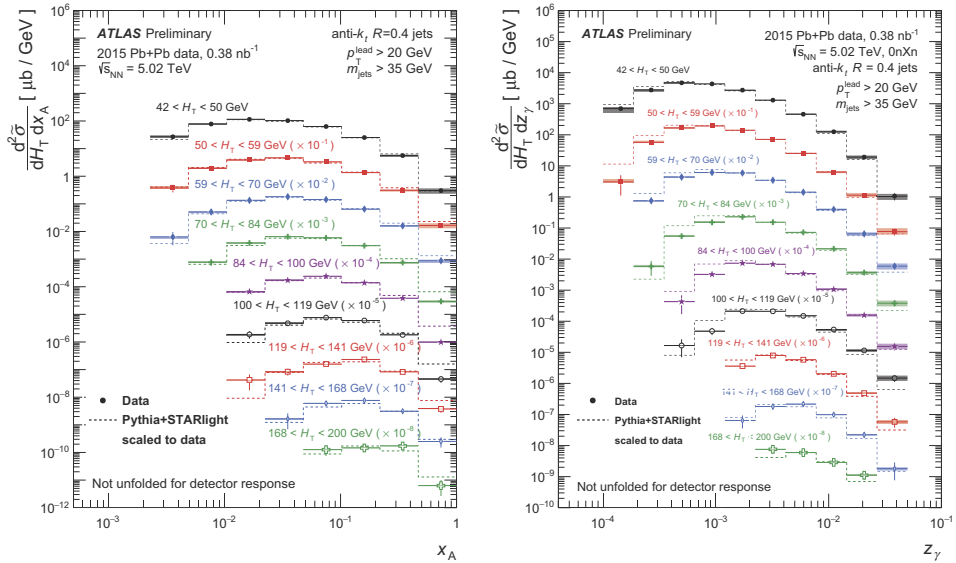


Fig. 1. Double-differential cross-sections $d^2\sigma/dH_T dx_A$ as a function of x_A (left) and $d^2\sigma/dH_T dz_\gamma$ as a function of z_γ (right) for different bins of H_T . The cross-sections are scaled by successive powers of 10 to improve visibility. The dashed lines represent the cross-section from PYTHIA+STARLIGHT scaled to have the same integral as the data within the fiducial region of the measurement.

References

- [1] A. H. Mueller, J. Qiu, Gluon Recombination and Shadowing at Small Values of x , Nucl. Phys. B268 (1986) 427–452.
- [2] I. Balitsky, Operator expansion for high-energy scattering, Nucl. Phys. B463 (1996) 99–160.
- [3] Y. V. Kovchegov, Small x F(2) structure function of a nucleus including multiple pomeron exchanges, Phys. Rev. D60 (1999) 034008.
- [4] R. Vogt, Jet photoproduction in peripheral heavy-ion collisions (2004). arXiv:hep-ph/0407298.
- [5] M. Strikman, R. Vogt, S. N. White, Probing small x parton densities in ultraperipheral AA and pA collisions at the LHC, Phys. Rev. Lett. 96 (2006) 082001.
- [6] S. Chekanov, et al., Dijet photoproduction at HERA and the structure of the photon, Eur. Phys. J. C23 (2002) 615–631.
- [7] C. Adloff, et al., Measurement of dijet cross-sections in photoproduction at HERA, Eur. Phys. J. C25 (2002) 13–23.
- [8] ATLAS Collaboration, Photo-nuclear dijet production in ultra-peripheral Pb+Pb collisions. ATLAS-CONF-2017-011. URL <https://cds.cern.ch/record/2244822>.
- [9] M. Cacciari, G. P. Salam, G. Soyez, The anti- k_t jet clustering algorithm, JHEP 04 (2008) 063. arXiv:0802.1189.
- [10] ATLAS Collaboration, The ATLAS Experiment at the CERN Large Hadron Collider, JINST 3.
- [11] T. Sjostrand, S. Mrenna, P. Z. Skands, PYTHIA 6.4 Physics and Manual, JHEP 0605 (2006) 026. arXiv:hep-ph/0603175.
- [12] P. Z. Skands, Tuning Monte Carlo Generators: The Perugia Tunes, Phys. Rev. D82 (2010) 074018.
- [13] G. A. Schuler, T. Sjostrand, Low and high mass components of the photon distribution functions, Z. Phys. C68 (1995) 607–624.
- [14] G. A. Schuler, T. Sjostrand, Parton distributions of the virtual photon, Phys. Lett. B376 (1996) 193–200.
- [15] GEANT4 Collaboration, S. Agostinelli et al., GEANT4: A simulation toolkit, Nucl. Instrum. Meth. A 506 (2003) 250–303.
- [16] ATLAS Collaboration, The ATLAS Simulation Infrastructure, Eur. Phys. J. C70 823–874.
- [17] S. R. Klein, J. Nystrand, J. Seger, Y. Gorunov, J. Butterworth, STARlight: A Monte Carlo simulation program for ultra-peripheral collisions of relativistic ions, Comput. Phys. Commun. 212 (2017) 258–268.
- [18] ATLAS Collaboration, Rapidity gap cross sections measured with the ATLAS detector in pp collisions at $\sqrt{s} = 7$ TeV, Eur. Phys. J. C72 (2012) 1926.
- [19] ATLAS Collaboration, Jet energy measurement and its systematic uncertainty in proton-proton collisions at $\sqrt{s} = 7$ TeV with the ATLAS detector, Eur. Phys. J. C75 (2015) 17.
- [20] ATLAS Collaboration, Jet energy scale and its uncertainty for jets reconstructed using the ATLAS heavy ion jet algorithm. ATLAS-CONF-2015-016. URL <https://cds.cern.ch/record/2008677>.